ACS Infectious Diseases

Letter

pubs.acs.org/journal/aidcbc

5-Fluoroimidazo[4,5-*b*]pyridine Is a Privileged Fragment That Conveys Bioavailability to Potent Trypanosomal Methionyl-tRNA Synthetase Inhibitors

Zhongsheng Zhang,[†] Cho Yeow Koh,[†,#] Ranae M. Ranade,[‡] Sayaka Shibata,[†] J. Robert Gillespie,[‡] Matthew A. Hulverson,[‡] Wenlin Huang,[†] Jasmine Nguyen,[†] Nagendar Pendem,[⊥] Michael H. Gelb,[⊥] Christophe L. M. J. Verlinde,[†] Wim G. J. Hol,[†] Frederick S. Buckner,[*,‡] and Erkang Fan[*,†]

[†]Department of Biochemistry, University of Washington, 1705 N.E. Pacific Street, Seattle, Washington 98195, United States

[‡]Department of Medicine, Division of Allergy and Infectious Diseases, and the Center for Emerging and Re-emerging Infectious Diseases (CERID), University of Washington, 750 Republican Street, Seattle, Washington 98109, United States

[⊥]Department of Chemistry, Bagley Hall, University of Washington, Seattle, Washington 98195, United States

Supporting Information

ABSTRACT: Fluorination is a well-known strategy for improving the bioavailability of drug molecules. However, its impact on efficacy is not easily predicted. On the basis of inhibitor-bound protein crystal structures, we found a beneficial fluorination spot for inhibitors targeting methionyl-tRNA synthetase of *Trypanosoma brucei*. In particular, incorporating 5-fluoroimidazo[4,5-*b*]pyridine into inhibitors leads to central nervous system bioavailability and maintained or even improved efficacy.

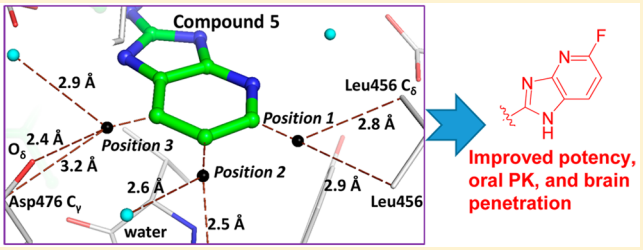

KEYWORDS: *human African trypanosomiasis, methionyl-tRNA synthetase, fluorination, bioavailability, brain penetration*

Human African trypanosomiasis (HAT), or sleeping sickness, is a devastating disease caused by infection with *Trypanosoma brucei*, a protozoan parasite that is transmitted to humans by the bite of an infected tsetse fly.[1,2] Two subspecies, *T. b. gambiense* and *T. b. rhodesiense*, cause human disease and put about 70 million people in sub-Saharan Africa at risk, according to the World Health Organization (WHO).[3,4] HAT progresses in two stages: the early hemolymphatic stage and the late stage when parasites cross the blood−brain barrier and invade the central nervous system (CNS). If untreated, late-stage infection is universally fatal. Current treatment options for HAT are inadequate. The two drugs for the early-stage infection, pentamidine and suramin, have considerable toxicity and require injection, although most patients at this stage can take oral medicine. For late-stage HAT, the arsenical drug melarsoprol causes 3−10% fatal encephalopathy during treatment and requires injection.[3] Despite this toxic effect, melarsoprol remains the frontline treatment because it is the only medicine available for treating late-stage *T. b. rhodesiense* infection. The other late-stage drug, eflornithine (used in combination with nifurtimox), is only useful for *T. b. gambiense* infection. Eflornithine also requires injection and is expensive to use. Clearly, orally and CNS available new effective therapeutics against both stages of HAT are urgently needed.

We have previously shown that methionyl-tRNA synthetase (MetRS) of *T. brucei* (*Tb*MetRS) is a validated drug target for the development of a new HAT treatment.[5,6] However, early analogues of inhibitors targeting bacterial MetRS[7,8] had poor oral bioavailability despite potent activity against parasite cells.[5] One way to address the bioavailability issue would be to discover alternative inhibitor scaffolds. Although we have identified urea-based *Tb*MetRS inhibitors with good oral and CNS availability, their potency against the parasites still needs improvement.[6] Another approach to improve bioavailability is through fluorination of compounds. It is well-known that fluorination of drug molecules may lead to improved metabolic stability and membrane permeability, resulting in desirable oral bioavailability and/or CNS exposure.[9,10] However, the effect of fluorination on the efficacy of a compound is less predictable. A study of a large number of matched-pair compounds showed that a change from H to F resulted in an activity enrichment factor of only 1.06 (in which no enrichment equals 1.00), and only 20−30% of the activity improvements were >2-fold.[11,12] Another study, involving library screening, indicates that fluorination generally leads to a loss of affinity,[13] unless one specifically screens for and identifies a protein environment that favors fluorinated compounds.[14] Therefore, a positive fluorination outcome in a drug discovery process still requires an extensive structure−activity relationship study.[10] In this paper, we show that only specific, not random, fluorination of *Tb*MetRS inhibitors leads to orally and CNS available

Received: March 7, 2016
Published: April 4, 2016

DOI: 10.1021/acsinfecdis.6b00036
ACS Infect. Dis. 2016, 2, 399−404

compounds with maintained or improved potency against the enzyme and the parasites. We also show that the best inhibitors in this study are active in murine models of *T. brucei* infection.

RESULTS AND DISCUSSION

We have reported many crystal structures of *Tb*MetRS in complex with inhibitors.[15,16] Recently, additional inhibitor-bound structures were obtained including a *Tb*MetRS complex with **5** (see the Supporting Information, Table S1 and Figure S1). These structures reveal how compounds such as **1**, **2**, and **5** interact with *Tb*MetRS (for compound structures, see Table 1). These potent inhibitors all bind to the target *Tb*MetRS similarly. The 3,5-dichlorophenyl moiety (Ar_1 in Figure 1A) occupies the enlarged methionine binding pocket, whereas the other aromatic moiety (Ar_2, such as quinolone in **1**, benzimidazole in **2**, and imidazo[4,5-*b*]pyridine in **5**) connected to Ar_1 through a linear linker occupies an auxiliary pocket observed only upon inhibitor binding.[15] The incorporation of benzimidazole or imidazopyridine moieties into MetRS inhibitors was reported earlier by GlaxoSmithKline scientists in attempts to improve the bioavailability compared to aminoquinolones.[8]

The auxiliary pocket is well filled by Ar_2, yet careful inspection of inhibitor-bound structures shows that placing a fluorine atom on the C5 position of the imidizopyridine ring of compound **5** might be favorable for affinity. At this position the F (dummy atom position 1 in Figure 1B) is predicted to interact with two C_δ methyl groups of Leu456 with distances of 2.8−2.9 Å, which are within distances observed for a C−F···H−C contact.[17,18] At the other two ring positions an F would be too close to a neighboring atom, which are a carbonyl oxygen or a carboxylate oxygen (dummy atom positions 2 and 3, Figure 1B). Oxygens are thought to interact unfavorably with carbon-bonded fluorine atoms.[19,20] In view of these short distances and the nature of contact atoms, these ring carbons are unlikely to accommodate a chlorine or methyl substitution in the observed binding mode. This analysis prompted us to test if a fluorine substitution on C5 of **5** (or equivalent position in **2**) might provide the desired benefits of conveying bioavailability, especially CNS penetration, while maintaining potency. A series of fluorinated and nonfluorinated compound pairs was synthesized and evaluated in several biological assays. The results are summarized in Table 1 and discussed below.

To assess the affinity of the inhibitors for the target *Tb*MetRS, we used a thermal shift binding assay[5] to rank order compounds. We did not use IC_{50} values against the *Tb*MetRS enzyme to rank compounds because most of the compounds reported in Table 1 are so potent that their IC_{50} values are close to or below the enzyme concentration used (see legend of Table 1). Those apparent IC_{50} values are valuable for indication of potency but are not useful for quantitative comparison (for enzyme inhibition data against both the *Tb*MetRS and the human mitochondrial MetRS for all compounds, see the Supporting Information). Compounds were also tested in a parasite growth inhibition assay.[5] Similar to previous observations,[5] the correlation between thermal shift (ΔT_m) and parasite growth inhibition (EC_{50}) is high for the data presented in Table 1 (R^2 is 0.84 for a linear relationship between ΔT_m and pEC_{50}). This high correlation supports the hypothesis that the compounds act on target and their cellular potency is directly related to their affinity to the target. This further supports using the thermal shift assay to rank the compounds' affinity for *Tb*MetRS. These inhibitors were tested

Table 1. Comparison of Fluorinated Compounds with Their Nonfluorinated Counterparts[a,b]

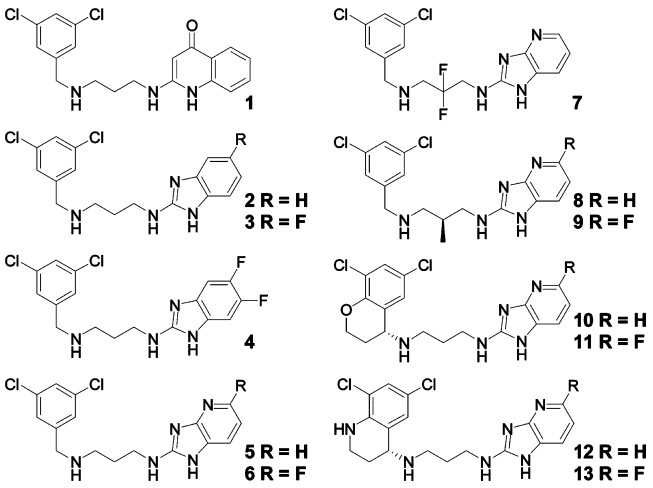

	ΔT_m on *Tb*MetRS (°C)[c]	*T. brucei* EC_{50} (nM)	Oral PK (50 mg/kg)		Brain to Plasma Ratio (%)
			C_{max} (μM)	$AUC_{0\text{-}8hr}$ (min*μM)	
1	21.6±0.0	3.7±0.3	0.73±0.20	110±24	0.17±0.17
2	17.5±0.1	50.4±1.2	0.38±0.04	62±5	ND[d]
3	16.4±0.2	101±7	ND	ND	ND
4	12.9±0.3	544±181	0.86±0.53	189±99	48.7±5.0
5	17.5±0.1	8.5±0.9	5.8±1.8	1466±435	2.4±0.7
6	18.9±0.1	5.3±0.9	24.9±4.9	4452±460	7.8±2.9
7	11.6±0.2	1227±334	4.0±1.5	710±52	1.6±0.1
8	15.9±0.1	9.7±1.7	ND	ND	ND
9	17.0±0.2	4.4 ±3.2	7.2±2.1	1218±105	2.0±1.1
10	22.5±0.1	5.0±0.8	ND	ND	ND
11	23.1±0.1	0.95±0.75	2.0±0.7	295±17	4.8±2.2
12	25.0±0.2	0.36±0.03	1.0±0.66	143±77	0.7±0.8
13	26.0±0.2	0.40±0.17	2.7±0.3	511±74	9.3±4.2

[a]White and gray background separates different groups of fluorinated and nonfluorinated compound analogues. [b]The values reported for ΔT_m and EC_{50} are the average ± SEM from two or more experiments. For PK and brain penetration experiments, the values are from one experiment with three mice per group. [c]Thermal shift assay is used for ranking on-target affinity, whereas enzyme inhibition data are available partially as previously published and in full in the Supporting Information. Compound **1** was used as a positive control in a recent

DOI: 10.1021/acsinfecdis.6b00036
ACS Infect. Dis. 2016, 2, 399−404

Table 1. continued

screen against *Tb*MetRS using an ATP depletion assay in 1536-well format with 35 nM enzyme (average IC_{50} = 24.2 nM),[21] whereas **1** and others (**2**, **5**, **6**, **10**, **11**, and **13**) were also reported for inhibition of *Tb*MetRS using an aminoacylation assay with 10 nM enzyme.[22] [d]ND, not determined.

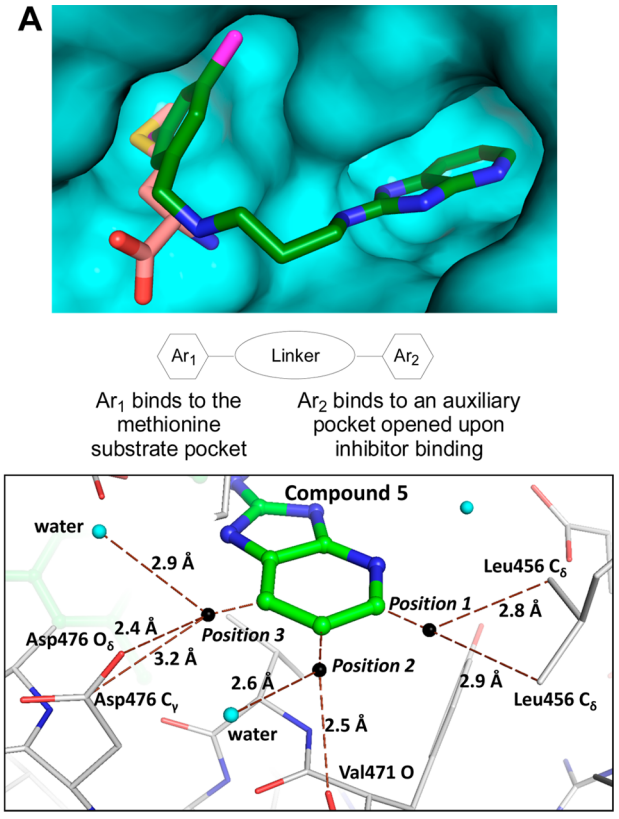

Figure 1. Binding of inhibitors to the *Tb*MetRS active site: (A) general inhibitor structural feature and the binding pose of **5** (carbons in green) superimposed to the binding pose of methionine (carbons in pink); (B) zoomed-in view of binding pocket for the Ar_2 portion showing potential sites of fluorination with dummy atoms (labeled as positions 1−3).

for host cell toxicity using CRL-8155 and Hep-G2 cell lines. Compounds **1** and **5**−**13** all yielded EC_{50} values close to or greater than 20 μM, whereas compounds **3** and **4** had EC_{50} values of ∼10 μM, and the starting compound **2** had an EC_{50} ∼ 5 μM. In addition, inhibitors were tested for oral pharmacokinetic (PK) properties and/or brain penetration in mice.

As shown in Table 1, compound **1** had a high affinity (ΔT_m = 21.6 °C under current assay conditions) and was potent against the parasite (EC_{50} = 3.7 nM). However, it had poor oral bioavailability with minimal brain exposure. The nonfluorinated compound **2** was less potent than **1** and lacked oral exposure. Fluorination at the 5-position of the benzimidazole ring produced compound **3**, which in theory could project the fluorine atom to dummy atom position 1 as revealed in Figure 1B. However, compound **3** lost affinity (lower ΔT_m) and potency (2-fold higher EC_{50}) compared to **2**. Adding more fluorine atoms to the benzimidazole ring (compound **4**) led to further loss of affinity and potency as one would expect from the unfavorable interactions at dummy atom position 2 in Figure 1B, although **4** had good brain penetration and slightly improved oral PK compared to **2**. Clearly, fluorination of the benzimidazole did not produce a desirable outcome.

In contrast, when fluorination was applied to the imidazopyridine analogues, dramatic changes were observed. The nonfluorinated starting compound **5** had good affinity for *Tb*MetRS and was potent against parasite cells (EC_{50} = 8.5 nM). Oral PK experiments showed higher plasma exposure of **5** than either **1** or **2** with low brain exposure (brain/plasma ratio of 2.4% at 60 min after ip dosing). A single fluorination at the 5-position of the imidazo[4,5-*b*]pyridine ring produced compound **6** with desirable effects on all assayed properties in Table 1 when compared to **5**. The affinity and potency of **6** improved over **5**, and, more importantly, oral PK data and brain permeability experiments confirmed ∼3-fold enhanced exposures of **6** compared to **5**. In comparison, a random fluorination at the linear linker region of **5** (compound **7**) led to major loss of affinity and inhibitory potency against parasite growth when compared to **5**. There was no improvement in oral PK or in brain penetration property either.

It thus appears that the 5-fluoroimidazo[4,5-*b*]pyridine moiety might be a privileged fragment for the series of *Tb*MetRS inhibitors under study with respect to conveying CNS bioavailability and maintaining or improving EC_{50} activity on *T. brucei*. To confirm this observation, we synthesized three more pairs of compounds for comparison (compounds **8** vs **9**, with additional modification in the linker region; and compounds **10** vs **11** and **12** vs **13**, with additional modifications in the Ar_1 region). The *S*-enantiomers of **8** and **9** were chosen because the (*R*)-enantiomer of **8** was ∼100-fold weaker in potency against *T. brucei* cells (data not shown). As shown in Table 1, the specifically fluorinated **9** and **11** were more potent than their nonfluorinated counter parts **8** and **10**, regardless of additional changes in the linker or the Ar_1 region with respect to **5**. The fluorinated compounds **9** and **11** were further profiled in oral PK and brain penetration experiments in mice. Overall, compounds **9** and **11** had less favorable properties than **6** regarding plasma or brain exposures. To further improve potency against the target enzyme and parasite cells, compound **13** and its nonfluorinated analogue **12** were synthesized, in which the dichloro-substituted chroman ring of **10** or **11** was replaced by a tetrahydroquinoline ring. This modification was based on a previously published study of bacterial MetRS inhibitors in which tetrahydroquinoline-containing inhibitors showed superior potency,[7] and specifically the *R*-enantiomer was more potent than the *S*-enantiomer.[8] Indeed, compound **13** demonstrated the highest affinity for *Tb*MetRS (Table 1). The nonfluorinated compound **12** has slightly less affinity for the *Tb*MetRS than **13** but is equally potent on parasite cells. However, its oral exposure is about a third of **13**'s, and its brain penetration was below the level of detection and thus much lower than **13**'s, confirming again the beneficial effects of the 5-fluoroimidazo[4,5-*b*]pyridine moiety. The PK profile and brain exposure of **13** showed higher exposure than **11**. Although the plasma exposure of **13** is about $^1/_{10}$ that of compound **6**, its 10-fold improvement in EC_{50} over **6** may compensate for the lower exposure. Compounds **6** and **13** were thus selected for testing in murine models of *T. brucei* infection.

In addition, we obtained crystal structures of *Tb*MetRS in complex with **6**−**8**, **11**, or **13** (see the Supporting Information, Table S1 and Figure S1). The structures confirmed that these fluorinated inhibitors bind to *Tb*MetRS as designed and

DOI: 10.1021/acsinfecdis.6b00036
ACS Infect. Dis. 2016, 2, 399−404

preserve almost exactly the binding modes seen for their nonfluorinated counter parts (Figure S2).

Compounds **6** and **13** were tested in a murine model of early-stage *T. brucei* infection. Mice (n = 4 per group) were infected with the STIB900 strain of *T. b. rhodesiense* at day 0, treated orally with compounds or vehicle from day 2 to day 5, and monitored for parasitemia in the blood until day 60. After the final day of treatment (day 5), mice were removed from the experiment if they were found to have microscopic parasitemia. The results (Table 2) show that control mice treated with vehicle all had parasitemia by day 6 and were euthanized. Compound **6** at the lowest dose did not cure, but at higher doses (20 and 50 mg/kg bid) produced partial cure. Encouragingly, compound **13** at every dose cured all treated mice. As a positive control, compound **14** (SCYX-7158, 4-fluoro-*N*-(1-hydroxy-3,3-dimethyl-2,1-benzoxaborol-6-yl)-2-(trifluoromethyl)benzamide)[23] cured four of four mice at 10 mg/kg and had partial or no cures at 5 or 1 mg/kg po bid, respectively.

Table 2. Survival of Mice in the Early-Stage *T. brucei* Infection Model

compound	dose (mg/kg) po bid for 4 days	cures as of day 60 (days of relapse)
6	50	2/4 (days 14, 14)
6	20	1/4 (days 10, 10, 10)
6	8	0/4 (days 5, 5, 6, 6)
13	50	4/4
13	20	4/4
13	8	4/4
14 (control)	10	4/4
14 (control)	5	1/4 (days 10, 14, 17)
14 (control)	1	0/4 (days 5, 5, 5, 5)
vehicle		0/4 (days 5, 5, 6, 6)

Given these positive results with **13** in the early-stage murine infection model, we performed another test of **6** and **13** in a late-stage model of infection using the *T. b. brucei* TREU667 strain that spreads to the CNS.[24,25] In this model, mice (n = 5 per group) were infected at day 0, and the infection was allowed to spread for 1 week. The mice were treated with either compounds or vehicle for 10 days from day 7 to day 16 (except treatment with diminazene as a control) and monitored for parasitemia for 90 days. There was no sign of toxicity from mice treated with either **6** or **13**. As shown in Figure 2, vehicle-treated mice all developed high parasitemia and were euthanized near the end of the treatment period. Compound **6** given orally at 50 mg/kg bid suppressed parasitemia during and for 4−5 days after treatment, but all mice showed detectable parasitemia and were sacrificed by day 24. Mice treated with **13** (50 mg/kg bid) showed longer survival days, and one of the five mice in the group was clear of infection at the end of the experiment. In the positive control group, mice treated with **14** (25 mg/kg qd) all survived and were free of infection at the end. In the diminazene control group, mice were treated with a single ip injection on day 7 at 10 mg/kg. It is well established that diminazene, which does not enter the CNS, completely clears parasites from the periphery, but any residual CNS parasites are able to re-establish bloodstream infection within a few weeks. In our model, the finding that the diminazene-treated group had recrudescent parasitemia and were euthanized between days 15 and 30 post-treatment matches published results of the late-stage *T. brucei* infection model.[23] Therefore, despite the lower efficacy of **13** than the positive control **14**, it is promising that compound **13** delayed parasite recrudescence and produced a partial cure of *T. brucei* infection in the CNS, without any signs of adverse effect on the mice.

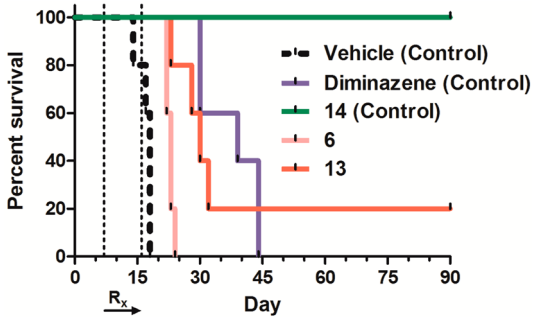

Figure 2. Survival of mice in the late stage *T. brucei* infection model. Mice were euthanized upon reappearance of parasitemia after treatment with compounds or vehicle.

In summary, we showed that specific fluorination and other modifications of initial inhibitors against *Tb*MetRS produced considerably improved properties over the starting compound. The improvements (**13** vs **5**) included a 20-fold decrease in EC_{50} and a 4-fold higher brain to plasma ratio (Table 1). The corresponding 5-fluoroimidazo[4,5-*b*]pyridine moiety was proven to be a privileged fragment for this series of inhibitors. Potent compounds bearing this functional group produced partial or complete cure in an early-stage *T. brucei* infection model and partial cure in a modified late-stage infection model. This suggests that further improvements of the *Tb*MetRS inhibitors may provide new orally and CNS available therapeutics for treating HAT.

METHODS

See the Supporting Information for chemical synthesis; protein purification and crystallography; thermal shift assay; enzyme inhibition assay and data; *T. brucei* growth inhibition assay; PK studies in mice; and distribution of compounds between mouse plasma and brain.

Early-Stage Infection Model. *T. brucei rhodesiense* STIB900 strain (isolate from a patient in Tanzania in 1982) was a gift of Simon Croft (London School of Hygiene and Tropical Medicine).[26] Female Swiss Webster mice (6−8 weeks of age, n = 4 per group) were injected ip with 200 μL of 1×10^4 bloodstream form parasites taken from fresh cultures and diluted in IMDM solution (day 0). Forty-eight hours postinfection (day 2), mice started receiving test compounds or vehicle (5% DMSO, 7% EtOH, 3% Tween-80 in saline). All mice were treated twice per day with test compounds or vehicle from day 2 to day 5 postinfection (eight doses). Doses for each compound are indicated in Table 2. Parasitemia was quantified microscopically from tail blood through day 60 postinfection.

Late-Stage Infection Model. The *T. brucei brucei* TREU667 strain (a gift from Dr. C. Bacchi, Pace University)[24,25] was harvested from a donor mouse, diluted in IMDM solution, and administered to experimental mice at a dose of 1×10^4 by ip injection (day 0). The subject animals were 6−8-week-old Swiss Webster female mice, n = 5 per group. Dosing with test compounds or vehicle began on day 7 postinfection. Dosing solution consisted of 5% DMSO, 7%

DOI: 10.1021/acsinfecdis.6b00036
ACS Infect. Dis. 2016, 2, 399−404

EtOH, and 3% Tween-80 in saline. A control group was given a single ip injection of diminazene on day 7 at 10 mg/kg in 200 μL. All other treatment groups were dosed orally for 10 days. Control compound **14** was given at 25 mg/kg once per day; **6** and **13** were given at 50 mg/kg twice per day; and the vehicle group received dosing solution twice per day. Two vehicle-treated mice died during the course of treatment due to the infection. The day after the end of treatment (day 17), the remaining vehicle-treated mice were all parasitemic and were removed from the experiment. The drug-treated mice had tail blood evaluated by microscopy at least twice a week for 30 days and then weekly out to 90 days postinfection. Mice with detectable parasites were euthanized and removed from the experiment.

All animal study protocols were approved by the Institutional Animal Care and Use Committee of the University of Washington (IACUC no. 4248-01).

■ ASSOCIATED CONTENT

Supporting Information

The Supporting Information is available free of charge on the ACS Publications website at DOI: 10.1021/acsinfecdis.6b00036.

Details of compound synthesis and characterization, protein production and crystallography, and the following biological assays: thermal shift assay, enzyme inhibition, parasite growth inhibition, PK studies in mice, and distribution of compounds between mouse plasma and brain (PDF)

Accession Codes

PDB codes for new structures reported in this work: 4ZT2, 4ZT3, 4ZT4, 4ZT5, 4ZT6, and 4ZT7.

■ AUTHOR INFORMATION

Corresponding Authors

*(F.S.B.) E-mail: fbuckner@uw.edu.

*(E.F.) E-mail: erkang@uw.edu.

Present Address

#(C.Y.K.) Department of Biological Sciences, National University of Singapore, Singapore 117543.

Author Contributions

All authors have given approval to the final version of the manuscript.

Notes

The authors declare no competing financial interest.

■ ACKNOWLEDGMENTS

Research reported in this publication was supported by the National Institute of Allergy and Infectious Diseases of the National Institutes of Health under Awards R01AI 084004 and R01AI 097177. The content is solely the responsibility of the authors and does not necessarily represent the official views of the National Institutes of Health. Crystallography performed in support of the work benefitted from remote access to resources at the Stanford Synchrotron Radiation Lightsource supported by the U.S. Department of Energy Office of Basic Energy Sciences under Contract DE-AC02-76SF00515 and by the National Institutes of Health (P41GM103393). We thank Stewart Turley and Robert Steinfeldt for maintaining crystallographic and computer equipment.

■ ABBREVIATIONS

AUC, area under the curve; bid, bis in die; CNS, central nervous system; HAT, human African trypanosomiasis; ip, intraperitoneal; MetRS, methionyl-tRNA synthetase; PK, pharmacokinetic; po, per os; qd, quaque die; SEM, standard error of the mean; WHO, World Health Organization

■ REFERENCES

(1) Hotez, P. J., Molyneux, D. H., Fenwick, A., Kumaresan, J., Sachs, S. E., Sachs, J. D., and Savioli, L. (2007) Current concepts − control of neglected tropical diseases. *N. Engl. J. Med. 357*, 1018−1027.

(2) Brun, R., Blum, J., Chappuis, F., and Burri, C. (2010) Human African trypanosomiasis. *Lancet 375*, 148−159.

(3) Trypanosomiasis, human African (sleeping sickness), http://www.who.int/mediacentre/factsheets/fs259/en/.

(4) Mapping the risk of human African trypanosomiasis, http://www.who.int/trypanosomiasis_african/country/risk_AFRO/en/.

(5) Shibata, S., Gillespie, J. R., Kelley, A. M., Napuli, A. J., Zhang, Z., Kovzun, K. V., Pefley, R. M., Lam, J., Zucker, F. H., Van Voorhis, W. C., Merritt, E. A., Hol, W. G., Verlinde, C. L., Fan, E., and Buckner, F. S. (2011) Selective inhibitors of methionyl-tRNA synthetase have potent activity against *Trypanosoma brucei* infection in mice. *Antimicrob. Agents Chemother. 55*, 1982−1989.

(6) Shibata, S., Gillespie, J. R., Ranade, R. M., Koh, C. Y., Kim, J. E., Laydbak, J. U., Zucker, F. H., Hol, W. G., Verlinde, C. L., Buckner, F. S., and Fan, E. (2012) Urea-based inhibitors of *Trypanosoma brucei* methionyl-tRNA synthetase: selectivity and in vivo characterization. *J. Med. Chem. 55*, 6342−6351.

(7) Jarvest, R. L., Berge, J. M., Berry, V., Boyd, H. F., Brown, M. J., Elder, J. S., Forrest, A. K., Fosberry, A. P., Gentry, D. R., Hibbs, M. J., Jaworski, D. D., O'Hanlon, P. J., Pope, A. J., Rittenhouse, S., Sheppard, R. J., Slater-Radosti, C., and Worby, A. (2002) Nanomolar inhibitors of *Staphylococcus aureus* methionyl tRNA synthetase with potent antibacterial activity against gram-positive pathogens. *J. Med. Chem. 45*, 1959−1962.

(8) Jarvest, R. L., Armstrong, S. A., Berge, J. M., Brown, P., Elder, J. S., Brown, M. J., Copley, R. C., Forrest, A. K., Hamprecht, D. W., O'Hanlon, P. J., Mitchell, D. J., Rittenhouse, S., and Witty, D. R. (2004) Definition of the heterocyclic pharmacophore of bacterial methionyl tRNA synthetase inhibitors: potent antibacterially active non-quinolone analogues. *Bioorg. Med. Chem. Lett. 14*, 3937−3941.

(9) Purser, S., Moore, P. R., Swallow, S., and Gouverneur, V. (2008) Fluorine in medicinal chemistry. *Chem. Soc. Rev. 37*, 320−330.

(10) Wang, J., Sánchez-Roselló, M., Aceña, J. L., del Pozo, C., Sorochinsky, A. E., Fustero, S., Soloshonok, V. A., and Liu, H. (2014) Fluorine in pharmaceutical industry: fluorine-containing drugs introduced to the market in the last decade (2001−2011). *Chem. Rev. 114*, 2432−2506.

(11) Dossetter, A. G., Griffen, E. J., and Leach, A. G. (2013) Matched molecular pair analysis in drug discovery. *Drug Discovery Today 18*, 724−731.

(12) O'Boyle, N. M., Boström, J., Sayle, R. A., and Gill, A. (2014) Using matched molecular series as a predictive tool to optimize biological activity. *J. Med. Chem. 57*, 2704−2713.

(13) Jordan, J. B., Poppe, L., Xia, X., Cheng, A. C., Sun, Y., Michelsen, K., Eastwood, H., Schnier, P. D., Nixey, T., and Zhong, W. (2012) Fragment based drug discovery: practical implementation based on ^{19}F NMR spectroscopy. *J. Med. Chem. 55*, 678−687.

(14) Vulpetti, A., Hommel, U., Landrum, G., Lewis, R., and Dalvit, C. (2009) Design and NMR-based screening of LEF, a library of chemical fragments with different local environment of fluorine. *J. Am. Chem. Soc. 131*, 12949−12959.

(15) Koh, C. Y., Kim, J. E., Shibata, S., Ranade, R. M., Yu, M., Liu, J., Gillespie, J. R., Buckner, F. S., Verlinde, C. L., Fan, E., and Hol, W. G. (2012) Distinct states of methionyl-tRNA synthetase indicate inhibitor binding by conformational selection. *Structure 20*, 1681−1699.

(16) Koh, C. Y., Kim, J. E., Wetzel, A. B., de van der Schueren, W. J., Shibata, S., Ranade, R. M., Liu, J. Y., Zhang, Z. S., Gillespie, J. R.,

Buckner, F. S., Verlinde, C. L. M. J., Fan, E. K., and Hol, W. G. J. (2014) Structures of *Trypanosoma brucei* methionyl-tRNA synthetase with urea-based inhibitors provide guidance for drug design against sleeping sickness. *PLoS Neglected Trop. Dis. 8*, e2775.
(17) Wang, Y., Callejo, R., Slawin, A. M. Z., and O'Hagan, D. (2014) The difluoromethylene (CF_2) group in aliphatic chains: synthesis and conformational preference of palmitic acids and nonadecane containing CF_2 groups. *Beilstein J. Org. Chem. 10*, 18−25.
(18) Dugovic, B., and Leumann, C. J. (2014) A 6′-fluoro-substituent in bicyclo-DNA increases affinity to complementary RNA presumably by CF−HC pseudohydrogen bonds. *J. Org. Chem. 79*, 1271−1279.
(19) Dunitz, J. D., and Taylor, R. (1997) Organic fluorine hardly ever accepts hydrogen bonds. *Chem.−Eur. J. 3*, 89−98.
(20) Zhou, P., Zou, J. W., Tian, F. F., and Shang, Z. C. (2009) Fluorine bonding − how does it work in protein-ligand interactions? *J. Chem. Inf. Model. 49*, 2344−2355.
(21) Pedró-Rosa, L., Buckner, F. S., Ranade, R. M., Eberhart, C., Madoux, F., Gillespie, J. R., Koh, C. Y., Brown, S., Lohse, J., Verlinde, C. L. M., Fan, E., Bannister, T., Scampavia, L., Hol, W. G. J., Spicer, T., and Hodder, P. (2015) Identification of potent inhibitors of the *Trypanosoma brucei* methionyl-tRNA synthetase via high-throughput orthogonal screening. *J. Biomol. Screening 20*, 122−130.
(22) Ranade, R. M., Zhang, Z. S., Gillespie, J. R., Shibata, S., Verlinde, C. L. M. J., Hol, W. G. J., Fan, E. K., and Buckner, F. S. (2015) Inhibitors of methionyl-tRNA synthetase have potent activity against *Giardia intestinalis* trophozoites. *Antimicrob. Agents Chemother. 59*, 7128−7131.
(23) Jacobs, R. T., Nare, B., Wring, S. A., Orr, M. D., Chen, D., Sligar, J. M., Jenks, M. X., Noe, R. A., Bowling, T. S., Mercer, L. T., Rewerts, C., Gaukel, E., Owens, J., Parham, R., Randolph, R., Beaudet, B., Bacchi, C. J., Yarlett, N., Plattner, J. J., Freund, Y., Ding, C., Akama, T., Zhang, Y. K., Brun, R., Kaiser, M., Scandale, I., and Don, R. (2011) SCYX-7158, an orally-active benzoxaborole for the treatment of stage 2 human African trypanosomiasis. *PLoS Neglected Trop. Dis. 5*, e1151.
(24) Jennings, F. W., Whitelaw, D. D., and Urquhart, G. M. (1977) The relationship between duration of infection with *Trypanosoma brucei* in mice and the efficacy of chemotherapy. *Parasitology 75*, 143−153.
(25) Bacchi, C. J., Nathan, H. C., Clarkson, A. B., Jr., Bienen, E. J., Bitonti, A. J., McCann, P. P., and Sjoerdsma, A. (1987) Effects of the ornithine decarboxylase inhibitors DL-α-difluoromethylornithine and α-monofluoromethyldehydroornithine methyl ester alone and in combination with suramin against *Trypanosoma brucei brucei* central nervous system models. *Am. J. Trop. Med. Hyg. 36*, 46−52.
(26) Kaiser, M., Bray, M. A., Cal, M., Bourdin Trunz, B., Torreele, E., and Brun, R. (2011) Antitrypanosomal activity of fexinidazole, a new oral nitroimidazole drug candidate for treatment of sleeping sickness. *Antimicrob. Agents Chemother. 55*, 5602−5608.

DOI: 10.1021/acsinfecdis.6b00036
ACS Infect. Dis. 2016, 2, 399−404